Flood wave propagation in steep mountain rivers

Gabriella Petaccia, Luigi Natale, Fabrizio Savi, Mirjana Velickovic, Yves Zech and Sandra Soares-Frazão

ABSTRACT

Most of the recent developments concerning efficient numerical schemes to solve the shallow-water equations in view of real world flood modelling purposes concern the two-dimensional form of the equations or the one-dimensional form written for rectangular, unit-width channels. Extension of these efficient schemes to the one-dimensional cross-sectional averaged shallow-water equations is not straightforward, especially when complex natural topographies are considered. This paper presents different formulations of numerical schemes based on the HLL (Harten–Lax–van Leer) solver, and the adaptation of the topographical source term treatment when cross-sections of arbitrary shape are considered. Coupled and uncoupled formulations of the equations are considered, in combination with centred and lateralised source term treatment. These schemes are compared to a numerical solver of Lax Friedrichs type based on a staggered grid. The proposed schemes are first tested against two theoretical benchmark tests and then applied to the Brembo River, an Italian alpine river, firstly simulating a steady-state condition and secondly reproducing the 2002 flood wave propagation.

Key words | 1D models, complex topography, shallow water equations, source terms, steady and unsteady flow

Gabriella Petaccia (corresponding author)
Luigi Natale
Department of Civil Engineering and Architecture,
University of Pavia, Via Ferrata, 1, 27100, Pavia,
Italy
E-mail: *petaccia@unipv.it*

Fabrizio Savi
Department of Hydraulics,
Transportation and Highways,
University of Roma 'La Sapienza',
Via Eudossiana 18, 00184, Rome,
Italy

Mirjana Velickovic
Fonds pour la Recherche dans l'Industrie et l'Agriculture (FRIA), B-1000 Brussels,
Belgium

Mirjana Velickovic
Yves Zech
Sandra Soares-Frazão
Université catholique de Louvain,
Institute of Mechanics,
Materials and Civil Engineering, Hydraulics Unit,
Place du Levant, 1, B-1348 Louvain-la-Neuve,
Belgium

INTRODUCTION

Mathematical simulation of flood wave propagation in rivers is a key tool for natural hazard studies. Nowadays the one-dimensional shallow water model is still widely used in field studies instead of more detailed two-dimensional models. This is due to practical and economical reasons: in fact the acquisition of the river topography is the very cost of flood propagation studies, the numerical simulation represents a minor cost. Usually ground surveys are used to model the geometry of mountain rivers since the cost of high precision light detection and ranging (LiDAR) surveys and of image post processing, needed to identify the bare soil, is seldom justified. Then, the airborne survey of large alluvial rivers requires an integrative bathymetric survey of the submerged riverbed and the total cost of the study would become unaffordable when very long river reaches have to be considered. So, we can consider that 1D models are still profitable for many real world applications.

Applications of 1D unsteady flow models to real world situations can be found in classical textbooks, such as Mahmood & Yevjevich (1975) and Cunge *et al.* (1980), or in recent scientific literature where rivers with rather mild slopes and slowly varying cross-sections are considered (Yoshida & Dittrich 2002; Helmio 2005; Remo & Pinter 2007; He *et al.* 2008; Wright *et al.* 2008).

The studies mentioned above generally consider rivers flowing in alluvial plains; nonetheless hydraulic studies for evaluation of natural hazard in newly proposed development areas are becoming of paramount importance in many European countries. Indeed, mountain valleys have been densely inhabited for centuries: the population, who in ancient time feared inundations and settled on the mountainside, is now compelled to use the bottom of the valley due to lack of space suitable for urban development.

doi: 10.2166/hydro.2012.122

To cope with the simulation of flood propagation in mountain rivers, the model should be capable of calculating unsteady flows presenting transcritical regime in a very irregular bed with abrupt shape changes, adverse-slope reaches and chutes.

When transcritical flow occurs, the shallow-water equations (SWE) need to be solved using algorithms which can handle discontinuities such as transonic/transcritical flows and propagating shocks. Many authors refer to Godunov-type schemes (Godunov 1959; Roe 1981; Le Veque 1998; Alcrudo & Garcia Navarro 1992; Hirsh 1992; Glaister 1993; Savic & Holly 1993; Toro 2009).

The results of these schemes are often presented for very simple geometries (rectangular and horizontal channels), while the applications to complicated topographies still need some work (Garcia Navarro *et al.* 1999; Wang *et al.* 2000; Ying *et al.* 2004). Indeed, in such cases the source terms, e.g. bed topography and bed resistance, play the most important role (Garcia Navarro & Vasquez Cendon 2000). In flows over irregular topographies, common algorithms tend to balance incorrectly the hydrostatic force acting on the lateral and bottom boundaries of the finite volume considered (Capart *et al.* 2003).

To address these problems, Hubbard & Garcia Navarro (2000) presented upwind schemes with decomposed source terms applied to one-dimensional open channel flow cases with general non-prismatic and non-rectangular geometries. These schemes were later extended by Vukovic & Sopta (2003). Liang & Marche (2009) developed a well-balanced numerical scheme for simulating frictional shallow flows over complex domains involving wetting and drying, solving the equations in a Godunov-type finite-volume framework, considering pressure balancing. They showed that non-negative reconstruction of Riemann states and compatible discretization of slope source term produce stable and well-balanced solutions to shallow flow hydrodynamics over complex topography.

The concept of well-balanced scheme was first introduced by Greenberg & Le Roux (1996) with a numerical scheme adapted to a scalar conservation law that preserves the balance between source terms and internal forces. However, the principle of well-balanced schemes, without naming it explicitly, was already explored earlier by Roe (1987). Later the concept was extended to more general hyperbolic systems. Lhomme & Guinot (2007) proposed an approximate Riemann solver for the solution of the hyperbolic systems of conservation laws with source terms, taking into account the source terms in the governing equations for the Riemann invariants. Finaud-Guyot *et al.* (2010) then introduced PorAs, a new approximate-state Riemann solver, to solve problems involving topography- and porosity-driven source terms. These schemes were applied to the shallow water equations, comparing the results with the classical HLLC (Harten–Lax–van Leer–Contact) solver and showing the improvement obtained with the new schemes.

Lee & Wright (2010) proposed a simple and efficient method to solve the one-dimensional shallow water equations with source terms, with a homogeneous form of the shallow water equations and a modification of well-known conservative numerical schemes to solve the new form of the equations. This modification to the homogeneous form combines the source term with the flux term. As a result, the source terms are automatically discretized to achieve perfect balance with the flux term without any special treatment and the method does not introduce numerical errors. The proposed method is verified against several benchmark tests and shows strong agreement with the analytical solutions.

Moving to a higher order of accuracy, Tseng (2004) proposed a scheme based on the finite-difference flux-limited total variation diminishing (TVD) and developed a simple approach to handle the source terms for the one-dimensional open channel flow simulation with rapidly varying bed topography. Caleffi *et al.* (2006) proposed a well-balanced central weighted essentially non-oscillatory (CWENO) method, fourth-order accurate in space and time, for shallow water system of balance laws with bed slope source term, extending the applicability of the standard CWENO scheme to very irregular bottoms, preserving high-order accuracy. Vignoli *et al.* (2008) presented a high-order ADER (Arbitrary high-order schemes using DERivatives) numerical scheme for solving the one-dimensional shallow water equations with irregular bed elevation. The governing equations are expressed in terms of water level, instead of water depth, and discharge. Non-oscillatory results are obtained for discontinuous solutions both for steady and unsteady cases. The resulting schemes

can be applied to solve realistic problems characterized by uneven bottom topography.

However, all these research efforts have generally focused on the shallow-water equations written for a unit-width channel, i.e. with the simplified variables h and $q = uh$ (Tseng 2004; Caleffi *et al.* 2006; Liang & Marche 2009; Xing & Shu 2011; Pu *et al.* 2012). Extension to the cross-section averaged equations, i.e. with the variables A and $Q = AV$ is not straightforward. This issue is addressed in the present work.

Moreover it has to be pointed out that the greatest part of the numerical schemes discussed above do not evaluate realistic discharges even if applied to almost simple cases.

The present work is focused on testing the suitability of some one-dimensional first-order accurate finite-volume schemes to a real-world case study, highlighting what difficulties arise when very irregular topographies are considered. This paper suggests a way of overcoming these shortcomings that can arise in practical applications and that are seldom shown in scientific literature.

The tested schemes consist of a finite-difference scheme and different finite-volume schemes with HLL (Harten–Lax–van Leer) fluxes computation. The topographical source terms are written in coupled or uncoupled form and these terms are discretized either in centred or lateralized form. As a very challenging case, because of the steep slope and abruptly changing cross-sections, the Brembo River was chosen to compare the numerical schemes. First, a steady flow analysis is performed to highlight the difficulties posed by the Brembo River case study and a modification to the classical mass flux expression is proposed to overcome the observed problems. Finally, a severe flood is simulated and the results are discussed and compared to field measurements.

THE BREMBO RIVER

The Brembo River is a 50.74 km long Alpine river located in Northern Italy (Lombardy Region), see Figure 1. It is a tributary of the Adda River that flows from Como Lake to the Po River. It is a very challenging river. Because of the many singularities of its riverbed – steep and adverse slopes

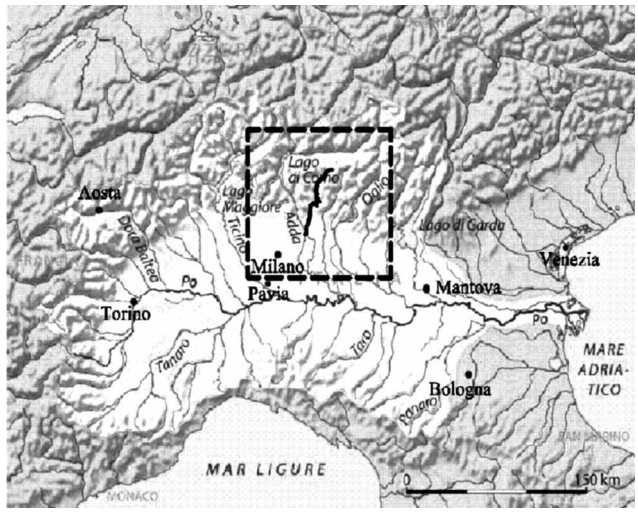

Figure 1 | Brembo River location.

(Figure 2), control structures and check dams, successive enlargements and constrictions (for example width reductions of a factor 10 over a 100-metre distance) – the Brembo River is difficult to deal with and it is used here as a benchmark for validation of numerical methods.

On 25–28th November 2002, due to heavy rainfalls in this Alpine Region, a significant flood came down from the mountains to the Brembo and Adda rivers, inundating

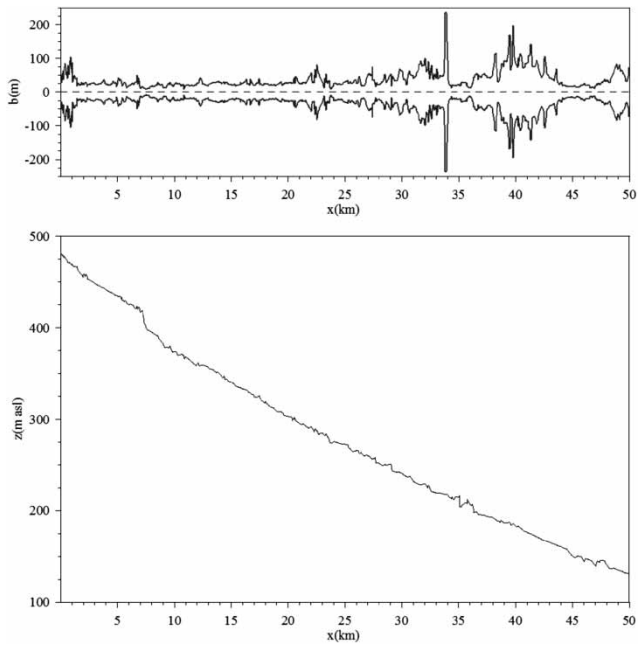

Figure 2 | Cross-section width, evaluated for $Q = 400\ m^3\ s^{-1}$, and bed profile along the thalweg.

a wide portion of the riverside and the city of Lodi. Due to the presence of many small mountain tributaries, the peak discharge along the Brembo River increased significantly from upstream to downstream. During the November 2002 event, at San Pellegrino gauging station a peak discharge of about 800 $m^3 s^{-1}$ was measured while about 1,100 $m^3 s^{-1}$ was measured further downstream, at Ponte Briolo (see Figure 3). After the flood event, maximum water elevations were measured in some points along the river.

A set of 274 cross-sections obtained by land survey defines the geometry of the river channel. The average distance between the cross-sections is 180 m. Values of Manning's coefficient n_M , ranging from 0.018 to 0.100 $m^{-1/3}$ s, were estimated from land-use maps, mean particle size of the river bed material and photographs of the riverbank revetments according to Arcement & Schneider (2001).

The flood hydrograph in the upstream section was reconstructed as illustrated in Figure 4, while the contribution of the numerous small mountain tributaries is considered as a distributed lateral inflow, and the downstream boundary condition is the stage-discharge relationship at the confluence with the Adda River.

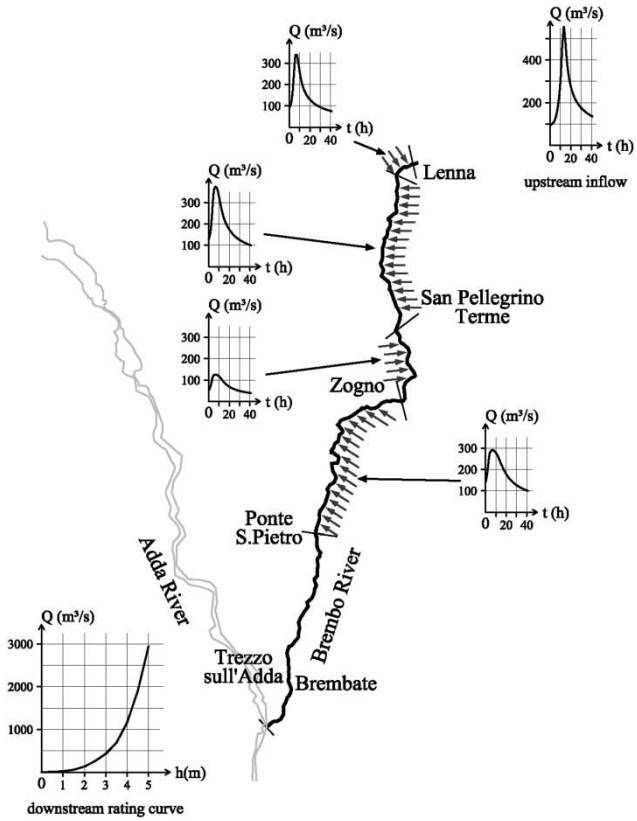

Figure 4 | Boundary conditions of the Brembo model: inflow hydrograph and stage-discharge relationship at the confluence with Adda river.

GOVERNING EQUATIONS

The model is based on the shallow-water equations written in conservative form (Cunge *et al.* 1980):

$$\frac{\partial \mathbf{U}}{\partial t} + \frac{\partial \mathbf{F}(\mathbf{U})}{\partial x} = \mathbf{S}(\mathbf{U}) \tag{1}$$

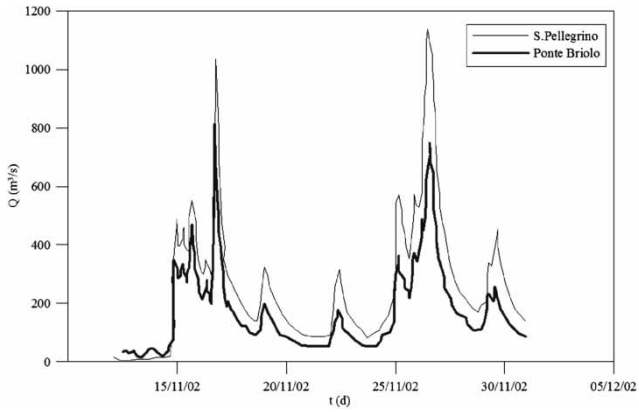

Figure 3 | Discharge measurement at San Pellegrino and Ponte Briolo stations.

where $\mathbf{U}$ is the vector of hydraulic variables, $\mathbf{F}$ the vector of fluxes, and $\mathbf{S}$ the vector of source terms. The vectors $\mathbf{U}$ and $\mathbf{F}$ are defined as

$$\mathbf{U} = \begin{pmatrix} A \\ Q \end{pmatrix}, \quad \mathbf{F}(\mathbf{U}) = \begin{pmatrix} Q \\ \frac{Q^2}{A} + gI_1 \end{pmatrix} = \begin{pmatrix} Q \\ \Sigma \end{pmatrix}, \tag{2}$$

where x is the spatial co-ordinate measured along the channel, t is the time, g is the gravitational acceleration, A is the cross-section wetted area, and Q is discharge. The term I_1 accounts for the hydrostatic pressure:

$$I_1 = \int_0^h (h - \eta) b(\eta) \mathrm{d}\eta \tag{3}$$

where b is the cross-section width at a given level η above the thalweg and h is the water depth (Figure 5).

Two different forms for the vector $\mathbf{S}(\mathbf{U})$ in (1) were analyzed. The first one, that will be referred

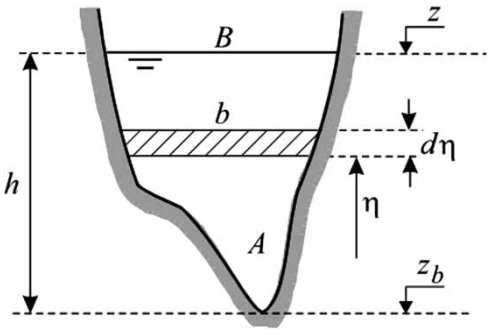

Figure 5 | Definition of the variables linked to *I*1 and *I*2.

to as the *uncoupled formulation* of the momentum equation is

$$\mathbf{S}(\mathbf{U}) = \begin{pmatrix} 0 \\ gA(S_0 - S_f) + gI_2 \end{pmatrix} = \begin{pmatrix} 0 \\ S_u \end{pmatrix} \tag{4}$$

where S_u denotes the uncoupled source term formulation, S_0 is the bed slope and S_f is the friction slope calculated by Manning's formula as:

$$S_f = \frac{n_M^2 V^2}{R^{4/3}} \tag{5}$$

where V is the averaged velocity and R the hydraulic radius. The function I_2 accounts for the width-variation effects:

$$I_2 = \int_0^h (h - \eta) \frac{\partial b(\eta)}{\partial x} d\eta \tag{6}$$

where the topography varies smoothly, the respective contributions of the bottom slope and cross-section width variations can be determined without problems.

The second form of the vector $\mathbf{S}(\mathbf{U})$ is an alternative form that is more suited where the bottom slope is not clearly defined, due to the irregular shape of the cross-sections. This formulation will be addressed in the following as the *coupled formulation*, already introduced by Cunge *et al.* (1980). It is obtained as follows. Through Leibniz integral rule for differentiation of a definite integral whose limits are functions of the differential variable, and considering expression (6) defining I_2, the derivative of I_1 expressed as (3) may be obtained as:

$$\frac{\partial I_1}{\partial x} = A \frac{\partial h}{\partial x} + I_2 \tag{7}$$

If the derivative of I_1 is taken for a constant water level $\bar{z}$, we obtain:

$$\left.\frac{\partial I_1}{\partial x}\right|_{\bar{z}} = I_2 + AS_0 \tag{8}$$

Substituting expression (8) in the momentum equation we obtain the coupled form of the source term (Soares-Frazão 2002; Capart *et al.* 2003)

$$\mathbf{S}(\mathbf{U}) = \begin{pmatrix} 0 \\ -gAS_f + g\left.\frac{\partial I_1}{\partial x}\right|_{\bar{z}} \end{pmatrix} = \begin{pmatrix} 0 \\ S_c \end{pmatrix} \tag{9}$$

where S_c denotes the coupled source term formulation. Following the definition in (7), I_2 will be calculated in the following as the derivative of I_1 for a constant water depth $\bar{h}$ (i.e. $\partial h/\partial x = 0$).

$$I_2 = \left.\frac{\partial I_1}{\partial x}\right|_{\bar{h}} - A\left.\frac{\partial h}{\partial x}\right|_{\bar{h}} = \left.\frac{\partial I_1}{\partial x}\right|_{\bar{h}} \tag{10}$$

NUMERICAL SCHEMES

Finite-difference scheme: SANA

This numerical scheme consists of a semi-implicit first-order scheme applied on a staggered grid (Figure 6): the wetted area A_i is defined at nodes i while the discharge $Q_{i+1/2}$ is defined at mid-distance between the nodes. This scheme, that has a structure similar to the Abbott-Ionescu scheme (Abbot & Ionescu 1967), was developed by Natale & Savi (1992) modifying the scheme proposed by Sielecki (1968). It is intuitive from the physical point of view and easy to implement (Petaccia & Savi 2002).

The momentum equation in (1) with the uncoupled source term formulation S_u is solved in a fully explicit

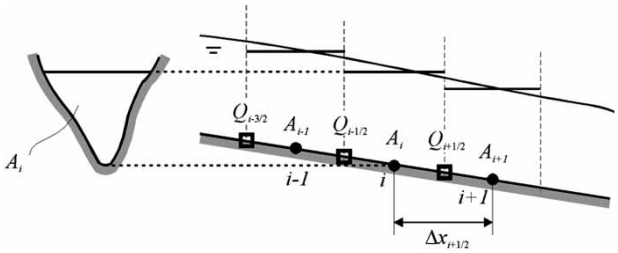

Figure 6 | The finite-difference scheme.

way, except for the source term:

$$Q_{i+1/2}^{n+1} = Q_{i+1/2}^{n} - \Delta t M_{i+1/2}^{n} - \frac{\Delta t}{\Delta x_{i+1/2}}\left(gI_{1,i+1}^{n} - gI_{1,i-1}^{n}\right) + \Delta t S_{\mathrm{u},i+1/2}^{n*} \tag{11}$$

The term $M_{i+1/2}^{n}$ corresponds to the spatial derivative of the momentum flux $\partial/\partial x\left(Q^2/A\right)$. It is evaluated in a upstream way on $i+1/2$ for supercritical flows and in a centered way on $i+1/2$ for subcritical flows according to a parameter s that depends on the Froude number $\mathrm{Fr} = V/c$, where $c = \sqrt{gA/B}$ and B is the cross-section width at the free surface. This yields for $M_{i+1/2}^{n}$

$$M_{i+1/2}^{n} = \frac{1}{\left(x_{i+1/2+s} - x_{i-1/2}\right)}\alpha\left(\left.\frac{Q^2}{\hat{A}}\right|_{i+1/2+s}^{n} - \left.\frac{Q^2}{\hat{A}}\right|_{i-1/2}^{n}\right) \tag{12}$$

with

$$\hat{A}_{i+1/2}^{n} = 0.5\left(A_i^n + A_{i+1}^n\right) \tag{12a}$$

and

$$s = \left\{\begin{array}{ll} 0 & \text{if } \left|\mathrm{Fr}_{i+1/2}^{n}\right| \geq 1 \\ 1 & \text{if } \left|\mathrm{Fr}_{i+1/2}^{n}\right| < 1 \end{array}\right\} \tag{12b}$$

$$\alpha = \left\{\begin{array}{ll} 1 & \text{if } \mathrm{Fr}_{i+1/2}^{n} > 0 \\ -1 & \text{if } \mathrm{Fr}_{i+1/2}^{n} < 0 \end{array}\right. \tag{12c}$$

In the source term $S_{\mathrm{u},i+1/2}^{n^*}$ of (11), superscript n^* denotes that the friction term is evaluated in a mixed explicit and implicit way while the topographical source terms are evaluated in an explicit way. The friction term S_{f} is discretized as

$$S_{f_{i+1/2}}^{n^*} = \frac{n_M^2 Q_{i+1/2}^{n+1}\left|Q_{i+1/2}^{n+1}\right|}{\left(\hat{A}_{i+1/2}^{n}\right)^2\left(\hat{R}_{i+1/2}^{n}\right)^{4/3}} \tag{13a}$$

with

$$\hat{R}_{i+1/2}^{n} = 0.5\left(R_i^n + R_{i+1}^n\right) \tag{13b}$$

The topographical source terms are represented by means of the uncoupled formulation (4) and are discretized in $S_{i+1/2}^{n^*}$ in an explicit and centred way:

$$\left(gAS_0\right)_{i+1/2}^{n^*} = \left(-gA\frac{\partial z_b}{\partial x}\right)_{i+1/2}^{n^*} = -g\hat{A}_{i+1/2}^{n}\frac{z_{b,i+1} - z_{b,i}}{\Delta x_{i+1/2}} \tag{14a}$$

$$\left(gI_2\right)_{i+1/2}^{n^*} = g\left(\left.\frac{\partial I_1}{\partial x}\right|_{\bar{h}}\right)_{i+1/2}^{n^*} = g\frac{I_{1,i+1}\big|_{h_i} - I_{1,i}\big|_{h_i}}{\Delta x_{i+1/2}} \tag{14b}$$

where z_b is the bottom elevation. In (14b), I_2 is calculated as the derivative of I_1 for a constant water depth h_i according to (10) and (3).

Finally, the continuity equation is solved in an implicit way and reads

$$A_i^{n+1} = A_i^n - \frac{\Delta t}{\Delta x_i}\left(Q_{i+1/2}^{n+1} - Q_{i-1/2}^{n+1}\right) \tag{15}$$

Finite-volume schemes

System (1) is discretized over a domain divided into computational cells assuming constant values of the conserved variables A and Q over each cell (Figure 7(a)). In contrast to the previous finite-difference scheme where variables are defined at the nodes, the variables are defined here over an entire cell, as cell-averaged values. The governing equations are then solved by means of a first-order finite-volume scheme that can be written in vector form as

$$\mathbf{U}_i^{n+1} = \mathbf{U}_i^n - \frac{\Delta t}{\Delta x}\left(\mathbf{F}_{i+1/2}^{*} - \mathbf{F}_{i-1/2}^{*}\right) + \mathbf{S}_i{*}\Delta t \tag{16}$$

The unknowns are the variables at time level $n+1$, i.e. A_i^{n+1} and Q_i^{n+1}, assumed constant over the cell in a first-order scheme. The mass and momentum fluxes, $\mathbf{F}_{i-1/2}^{*}$ and

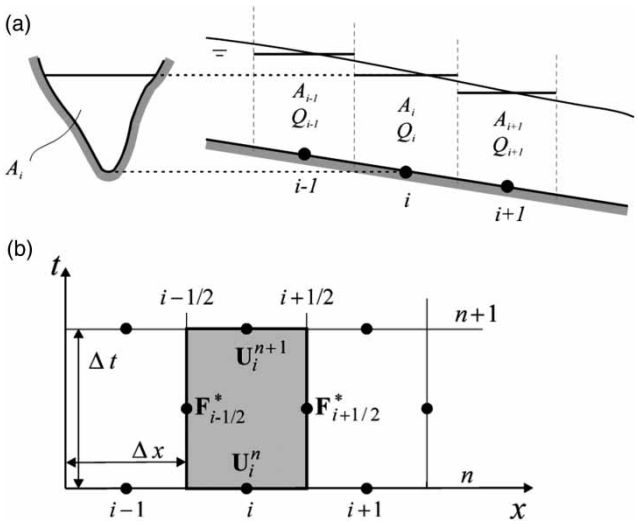

Figure 7 | (a) Spatial discretization; (b) definition of the variables in a *x*–*t* system.

$\mathbf{F}^*_{i+1/2}$, are calculated at the cell interfaces. Fluxes and topographical source term calculations are detailed in the next sections. It must be pointed out that here both the uncoupled formulation S_u and the coupled formulation S_c can be used for the source term. The friction term S_f is evaluated in a mixed explicit and implicit way as

$$S_{fi}^{n+1} = \frac{n^2 Q_i^{n+1}|Q_i^{n+1}|}{(A_i^n)^2 (R_i^n)^{4/3}} \tag{17}$$

Flux calculation by HLL solver

In the HLL scheme (Harten *et al.* 1983) the fluxes $\mathbf{F}^*$ at the interface between two computational cells are calculated as the solution of an approximate Riemann problem between two distinct constant states $\mathbf{U}_L$ at the left side and $\mathbf{U}_R$ at the right side (Figure 7(b)). Two waves of speed λ_L and λ_R, respectively, are issued from the initial discontinuity between $\mathbf{U}_L$ and $\mathbf{U}_R$. In the original HLL method, the solution is approximated as a constant intermediate state denoted $\mathbf{U}^*$ in the so-called star region between the two waves λ_L and λ_R. Following Toro (2009), the sought flux $\mathbf{F}^*$ in this star region is calculated as:

$$\mathbf{F}^* = \begin{cases} \mathbf{F}_L & \text{if} \quad \lambda_L \geq 0 \\ \mathbf{F}^{\mathrm{HLL}} \equiv \dfrac{\lambda_R \mathbf{F}_L - \lambda_L \mathbf{F}_R + \lambda_R \lambda_L (\mathbf{U}_R - \mathbf{U}_L)}{\lambda_R - \lambda_L} & \text{if} \quad \lambda_L \leq 0 \leq \lambda_R \\ \mathbf{F}_R & \text{if} \quad \lambda_R \leq 0 \end{cases} \tag{18}$$

with the wave speeds λ_L and λ_R defined following Toro (2001) by means of synthetic expressions accounting for both sub- and supercritical cases and including an entropy fix to handle the critical point where the Froude number Fr = 1:

$$\begin{aligned} \lambda_L &= V_L - c_L w_L \\ \lambda_R &= V_R + c_R w_R \end{aligned} \tag{19}$$

In (19), w_K ($K = L, R$) is a weight function given by:

$$w_K = \begin{cases} \sqrt{\dfrac{1}{2}\left(\dfrac{(h^* + h_K)h^*}{h_K^2}\right)} & \text{if} \quad h^* > h_K \\ 1 & \text{if} \quad h^* \leq h_K \end{cases} \tag{20}$$

Depth h^* is an estimate for the exact solution of h in the star region between the two waves λ_L and λ_R:

$$h^* = \frac{1}{g}\left(\frac{1}{2}(c_L + c_R) + \frac{1}{4}(V_L - V_R)\right)^2 \tag{21}$$

Numerical treatment for the uncoupled topographical source terms

The uncoupled topographical source terms correspond to the formulation (4) of the source term of the momentum equation, i.e. $gAS_0 + gI_2$. These terms, which are evaluated within the source term $\mathbf{S}_i^*$ of (16), can be discretized either in a centred way or in a lateralized way following the scheme proposed by Fraccarollo *et al.* (2003).

In the centred scheme, the spatial derivative is centred on cell i:

$$(gAS_0)_i = \left(-gA\frac{\partial z_b}{\partial x}\right)_i = -gA_i \frac{z_{b,i+1} - z_{b,i-1}}{2\Delta x} \tag{22a}$$

$$(gI_2)_i = g\left(\frac{\partial I_1}{\partial x}\bigg|_{\bar{h}}\right)_i = g\frac{I_{1,i+1}|_{h_i} - I_{1,i-1}|_{h_i}}{2\Delta x} \tag{22b}$$

As for (14b) in (22b), I_2 is calculated as the derivative of I_1 for a constant water depth h_i according to (10) and (3).

In lateralized schemes, weighting factors linked to the wave propagation speeds are applied to the topographical source term, resulting in a formulation close to an upwind

scheme (Bermudez & Vasquez 1994) for the momentum equation. In the lateralized scheme of Fraccarollo *et al.* (2003), denoted LHLL scheme, the derivatives are evaluated over the distance Δx between the two cell interfaces. The value of the variable at each interface is estimated in an upwind way, with weights λ_L and λ_R corresponding to the HLL wave-speed estimators (19). It must be noted that the values of λ_L and λ_R are distinct for the $i+1/2$ and $i-1/2$ interfaces

$$(gAS_0)_i = -\frac{g}{\Delta x}A_i\left[\left(\frac{\lambda_R z_{b,i}-\lambda_L z_{b,i+1}}{\lambda_R-\lambda_L}\right)_{i+1/2}-\left(\frac{\lambda_R z_{b,i-1}-\lambda_L z_{b,i}}{\lambda_R-\lambda_L}\right)_{i-1/2}\right] \tag{23a}$$

As in (22b), I_2 is calculated as the derivative of I_1 for a constant water depth $\bar{h}$

$$(gI_2)_i = \frac{g}{\Delta x}\left[\left(\frac{\lambda_R I_{1,i}|_{h_i}-\lambda_L I_{1,i+1}|_{h_i}}{\lambda_R-\lambda_L}\right)_{i+1/2}-\left(\frac{\lambda_R I_{i,i-1}|_{h_i}-\lambda_L I_{1,i}|_{h_i}}{\lambda_R-\lambda_L}\right)_{i-1/2}\right] \tag{23b}$$

Numerical treatment for the coupled topographical source terms

The coupled topographical source terms correspond to formulation (9) of the momentum equation, where the topographical effects are represented by the spatial derivative of I_1 at a constant level $\bar{z}$, i.e. $\partial/\partial x(gI_1)|_{\bar{z}}$.

As already outlined, coupling the topographical source terms as in (9) is more suited to natural topographies with steep slopes and severe variations of cross-section width. Again, this term can be discretized either in a centred or lateralized way.

In the centred scheme the spatial derivative is centred on cell i :

$$\left(\frac{\partial I_1}{\partial x}\Big|_{\bar{z}}\right)_i = \frac{I_{1,i+1}|_{\bar{z}_i}-I_{1,i-1}|_{\bar{z}_i}}{2\Delta x} \tag{24}$$

Using the LHLL approach of Fraccarollo *et al.* (2003), the discretization of the topographical source term in the lateralized scheme, reads:

$$\left(\frac{\partial I_1}{\partial x}\Big|_{\bar{z}}\right)_i = \frac{1}{\Delta x}\left(\left(\frac{\lambda_R I_{1,i}|_{z_i}-\lambda_L I_{1,i+1}|_{z_i}}{\lambda_R-\lambda_L}\right)_{i+1/2}-\left(\frac{\lambda_R I_{1,i-1}|_{z_i}-\lambda_L I_{1,i}|_{z_i}}{\lambda_R-\lambda_L}\right)_{i-1/2}\right) \tag{25}$$

As for the uncoupled source terms, this consists of evaluating the derivative over a distance Δx between the two cell interfaces. The value of $I_1|_{\bar{z}}$ at each interface is estimated in a lateralized way, with weights corresponding to the HLL discretization of the fluxes.

Boundary conditions

The boundary conditions considered for the applications consist of a prescribed discharge or hydrograph at the upstream end and a prescribed water level at the downstream end of the model. The treatment of the upstream boundary condition for the finite-difference model SANA and the finite-volume schemes are presented briefly.

For SANA, following (Natale *et al.* 2004), when flow is supercritical at the time level $n+1$, two conditions are required: here, the discharge and the upstream Froude number are provided as Q_{UB}^{n+1} and $\mathrm{Fr}_{\mathrm{UB}}^{n+1}$. From there, the hydraulic variables at the upstream boundary $Q_{1/2}^{n+1}$ and A_1^{n+1} are calculated as functions of the prescribed values using

$$Q_{1/2}^{n+1} = Q_{\mathrm{UB}}^{n+1} \quad \text{and} \quad \mathrm{Fr}_{\mathrm{UB}}^{n+1} = \frac{Q_{\mathrm{UB}\,1/2}^{n+1}}{A_1^{n+1}\sqrt{g\bar{h}_1}} \tag{26a}$$

where $\bar{h}_1$ is evaluated as A_1^{n+1}/B_1^{n+1}.

When the flow is subcritical only Q_{UB}^{n+1} is needed to obtain

$$Q_{1/2}^{n+1} = Q_{\mathrm{UB}}^{n+1} \tag{26b}$$

In this process, the geometry of the virtual section at the upstream boundary (position 1/2) has not to be defined explicitly. As illustrated in Figure 6, the cross-section is known at the locations i.

For the finite-volume schemes with HLL fluxes, we obtain, for supercritical flows

$$F^*_{1/2} = \begin{pmatrix} Q^{n+1}_{\mathrm{UB}} \\ \Sigma^{n+1}_{\mathrm{UB}} \end{pmatrix} \tag{27a}$$

where the momentum $\Sigma^{n+1}_{\mathrm{UB}} = f\left(Q^{n+1}_{\mathrm{UB}}, \mathrm{Fr}^{n+1}_{\mathrm{UB}}\right)$ is computed using the known geometry of section at position *1* and the prescribed discharge and Froude number. The treatment for subcritical flow is defined by means of the characteristics as (Soares-Frazão 2002):

$$F^*_{1/2} = \begin{pmatrix} Q^{n+1}_{\mathrm{UB}} \\ \Sigma^{n}_{1} + (v+c)^{n}_{1}\left(Q^{n+1}_{\mathrm{UB}} - Q^{n}_{1}\right) \end{pmatrix} \tag{27b}$$

The treatment of the downstream boundary conditions follows directly.

Summary of the tested schemes

A total of five schemes with different source term discretization have been tested: four of them use HLL numerical solver. All the tested schemes are capable of maintaining the water at rest when used on simple rectangular cross sections. The aim of this paper is to apply the considered schemes to irregular geometries.

For clarity, the code names of each scheme are summarised in Table 1. The discretization is either FV for finite-volumes following Equation (16) or FD for the finite-difference scheme of Equations (11)–(15). In the name of the scheme HLL-XX, the first X-letter U or C describes the source terms as uncoupled or coupled while the second X-letter stands for centred or lateralized.

Table 1 | Summary of numerical schemes

Name	Discretization	Source terms
SANA	FD	Centered
HLL-UC	FV	Centered
HLL-UL	FV	Lateralized
HLL-CC	FV	Centered
HLL-CL	FV	Lateralized

For all the tests that will follow, a constant value of CFL = 0.8 will be used to guarantee stability.

CLASSICAL VALIDATION TEST CASES

Bump

The schemes listed in Table 1 are applied to simulate steady flow in the well-known 'bump' test case that was proposed by Goutal & Maurel (1997) in the CADAM project – Concerted Action on Dam Break Modelling – (Soares-Frazão *et al.* 2000) and by many other researchers (Vazquez-Cendon 1999; Zhou *et al.* 2001; Valiani *et al.* 2002; Ying *et al.* 2004; Aricò & Tucciarelli 2007). One of the challenges of this test concerns the computed discharge: indeed, many first and second order accurate, one- and two-dimensional schemes fail in reproducing the constant discharge across the bump: see for example Schippa & Pavan (2008), Kuiry *et al.* (2008), Wang *et al.* (2011), Pu *et al.* (2012), and Ying & Wang (2008).

The shape of the bump is illustrated in Figures 8(a) and 8(b). A mesh interval of $\Delta x = 0.1$ m was used in the computations. A discharge $Q = 0.18\ \mathrm{m^3\,s^{-1}}$ was imposed at the upstream boundary and a water level of 0.33 m was specified as the downstream boundary condition. The case is frictionless, the initial water elevation is 0.33 m and the discharge is nil. The simulation continued until the steady state is achieved. The semi-analytical reference solution is given, for example, in Goutal & Maurel (1997) and is obtained by solving the Bernoulli equation.

For the sake of shortness of the paper, in Figures 8(a) and 8(b) the computed water-surface profile and energy grade line are compared to the analytical solution (black lines) only for SANA and HLL-CL schemes. All the computed results are in good agreement with the semi-analytical solution for the water level, regardless of the topographical source terms discretization, except for some irregularities at the beginning and at the end of the bump. Indeed, the water level is correctly predicted as well as the shock position, except for SANA (Figure 8(a)) that anticipates its location.

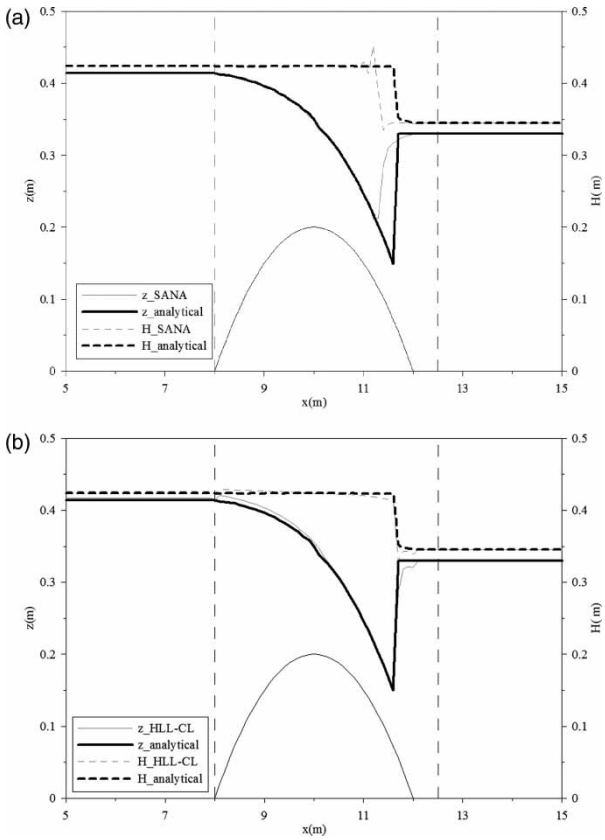

Figure 8 | (a) Water level (lower curve) and total head (upper dashed curve) for the bump test case: SANA (grey line) and analytical solution (black line). (b) Water level (lower curve) and total head (upper dashed curve) for the bump test case: HLL-CL (grey line) and analytical solution (black line).

However, the discharge is not perfectly constant with the consequence that the energy grade line is not well reproduced. This can be seen in Table 2 providing the mean square errors of water level, discharge and total head, computed across the bump for the portion of the flume between 8.0 and 12.5 m, as indicated in Figures 8(a) and 8(b) with the vertical lines. It is interesting to note that while SANA fails in computing the right position for the hydraulic jump, it reproduces perfectly the constant discharge.

Table 2 | Bump case. Mean square errors for the water level z_w, the computed discharge Q and the hydraulic head H

	SANA	HLL-UC	HLL-UL	HLL-CC	HLL-CL
z_w (m)	0.038	0.004	0.013	0.004	0.008
Q (m³/s)	0.000	0.008	0.010	0.008	0.008
H (m)	0.016	0.006	0.005	0.005	0.003

Water at rest

The schemes listed in Table 1 were then applied to verify the static equilibrium condition, testing the ability for the schemes to maintain water at rest over an irregular topography. As introduced by Vasquez-Cendon (1999), a necessary condition for the static equilibrium, also called *C*-property, is to perfectly balance the hydrostatic pressure term and the topographical source term.

A reach with a particularly uneven bed was chosen; the river's topography was modelled by 129 cross-sections, spaced approximately 50 m, with cross-sections width ranging from 40 to 321 m in 5.67 km, with abrupt changes in the bed slope (see Figure 9). The condition of water at rest was imposed with a water elevation of 490 m a.s.l. and wall boundary conditions at the upstream and downstream end. A constant Manning coefficient of 0.04 m $s^{-1/3}$ was adopted.

Among all the presented schemes only SANA is capable of keeping water at rest without giving unrealistic oscillations, as can be seen in Figure 10. This will be discussed in the next section.

CONSERVATIVE FORMULATION OF THE MASS FLUX

Among the pioneering work in the field of well-balanced schemes, Nujic (1995) proposed a simple and practical solution to avoid unrealistic oscillations of the free surface for water at rest on irregular topographies. His solution was developed for the 1D shallow-water equations written for unit-width rectangular channels. Although originally presented for Lax scheme, this solution has been adapted to most classical schemes (e.g. Capart *et al.* 2003; Lee & Wright 2010). Instead of considering the difference of the water depth in Equation (18) of the mass flux, he suggested to use the difference in water levels. For the HLL scheme, this would be:

$$q^* = \frac{\lambda_R q_L - \lambda_L q_R + \lambda_L \lambda_R \left(z_{w,R} - z_{w,L}\right)}{\lambda_R - \lambda_L} \tag{28}$$

with q^* the unit-width mass flux, q_L and q_R the unit-width discharges in the left and right cells, respectively, and $z_{w,L}$ and $z_{w,R}$ the corresponding water levels.

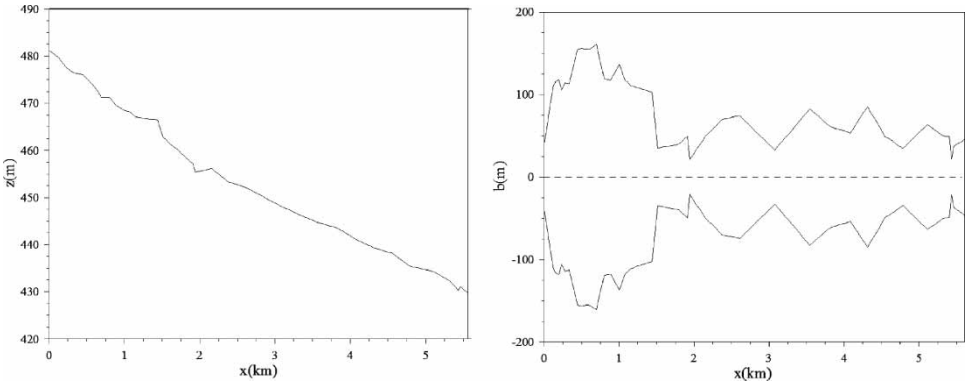

Figure 9 | Initial conditions for the water at rest test case.

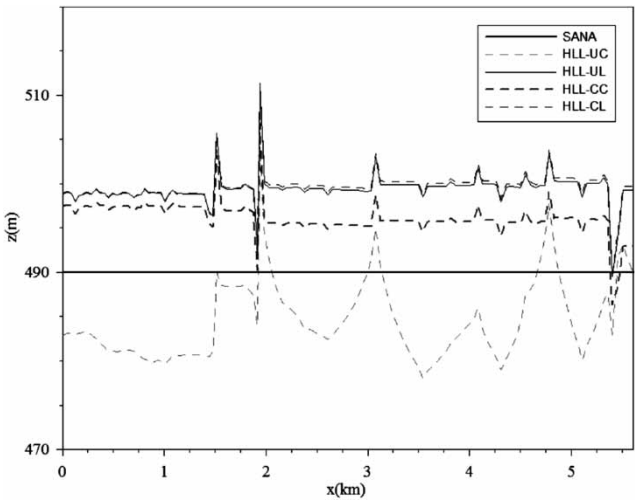

Figure 10 | Results for the water at rest test case.

The proposed solution consists of transposing this technique to the shallow-water equations written in terms of wetted area A and discharge Q. Following (18) the mass flux expression should be:

$$Q^* = \frac{\lambda_R Q_L - \lambda_L Q_R + \lambda_L \lambda_R (A_R - A_L)}{\lambda_R - \lambda_L} \tag{29}$$

As illustrated in Figure 11, significant variations are observed in the wetted area between two consecutive cross-sections with very comparable water levels. As a consequence, the large difference $(A_R–A_L)$ induces spurious variations of the computed mass flux (29) that results in a wrong balance of the mass conservation equation, leading to an incorrect computed water surface. The proposed

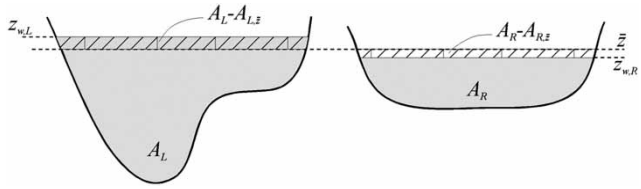

Figure 11 | Difference in wetted area.

transposition of Nujic's technique to (29) considers the difference of the hatched areas only. If we define $A_{L,\bar{z}}$ and $A_{R,\bar{z}}$ as the wetted area in cross-sections L and R respectively, calculated with the mean water level $\bar{z} = (z_{w,R} + z_{w,L})/2$, the expression for the mass flux becomes:

$$Q^* = \frac{\lambda_R Q_L - \lambda_L Q_R + \lambda_L \lambda_R \left[(A_R - A_{R,\bar{z}}) - (A_L - A_{L,\bar{z}}) \right]}{\lambda_R - \lambda_L} \tag{30}$$

Applying this modification to the four HLL schemes of Table 1 yields the results presented in Table 3. All schemes now reproduce the correct position of the hydraulic jump, with an improvement at the upstream and downstream ends of the bump. Figures 12 shows the results computed

Table 3 | Bump case. Mean square errors for the water level z_w, the computed discharge Q and the hydraulic head H computed according to (30)

	HLL-UC mod(30)	HLL-UL mod(30)	HLL-CC mod(30)	HLL-CL mod(30)
z_w (m)	0.014	0.004	0.008	0.004
Q ($m^3 s^{-1}$)	0.003	0.007	0.003	0.005
H (m)	0.003	0.006	0.003	0.004

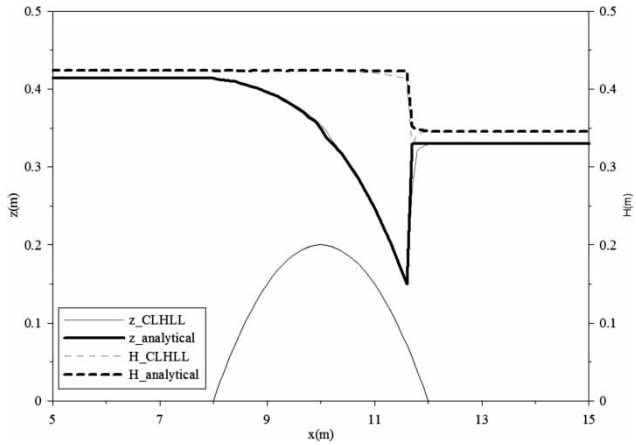

Figure 12 | Water level (lower curve) and total head (dashed upper curve) for the Bump case: HLL-CL modified according to (30) (grey line) and analytical solution (black line).

with the modified mass flux Equation (30) for the HLL-CL scheme applied to the bump case.

HLL-CC and HLL-CL schemes modified by Equation (30) reduce the errors in computed discharge. Also the calculated water profile and the energy grade line better match the reference solution.

Since the modification of Equation (30) brought significant improvements to the bump test case, it was also tested on the water at rest test case (see Figures 13(a) and 13(b)). The proposed modification improves the results for all the schemes even if the most significant improvement is found for HLL-CL that now keeps the water completely at rest.

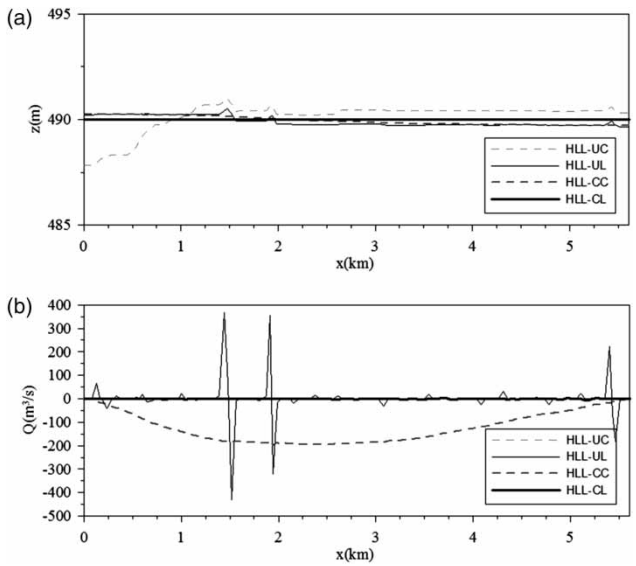

Figure 13 | (a) Water at rest with the improved mass flux. (b) Discharge with the improved mass flux.

The uncoupled formulations (HLL-UC and HLL-UL) do not satisfy the equilibrium condition when the cross-sections are very irregular, regardless of the discretization used for the topographical source terms. The reason is as follows: for water at rest, the momentum equation in system (1) with source term written with the uncoupled formulation (4) reduces to:

$$g\frac{\partial I_1}{\partial x} = gAS_0 + gI_2 \tag{31}$$

If the topography is very uneven, the discretization of (31) such as (22a–22b) or (23a–23b) will not provide the right balance. This reason was already invoked by Capart *et al.* (2003) to prefer the coupled formulation (9) in the case of irregular topography.

Regarding the coupled formulations (HLL-CC and HLL-CL), as introduced by Fraccarollo *et al.* (2003), only the lateralized discretization HLL-CL of the source term allows to perfectly balance the momentum equation (Soares-Frazão 2002). Indeed, in the HLL-CC scheme, the source term is discretized over $2\Delta x$, leading to an imbalance with the hydrostatic pressure terms in the momentum fluxes if the differences between the successive cross-sections are too important.

From the preceding results, it appears that the HLL-CL scheme with modification (30) is the most appropriate among the finite-volume schemes. This modified scheme will be from now on denoted CLHLL, the acronym standing for *Conservative Lateralized HLL* scheme.

BREMBO RIVER CASE STUDY: STEADY-STATE FLOW

To check the different considered numerical integration schemes of the SWE when applied to very uneven and steep water courses, a steady flow in the Brembo River is investigated. This steady flow is calculated by means of the unsteady flow schemes CLHLL, SANA and HLL-CL by imposing a constant discharge at the upstream boundary and starting from a dry bed initial condition.

The reference solution on the other hand is obtained by means of the steady-state version of HEC-RAS (Brunner 2002), which integrates the Energy equation with the standard step method and the Momentum equation to evaluate head losses (flow through bridges or culverts) and to locate hydraulic jumps. These steady-flow results were compared to the results obtained using the research code FRESCURE developed by Natale & Savi (1999) that is also based on the same equations. No differences were found between these two sets of steady-flow results, allowing the use of the HEC-RAS solution as a reference solution.

Steady-state simulations are run with a constant 400 $m^3 s^{-1}$ discharge – corresponding to the 35-year return period peak flood for the upstream station of Lenna – on the whole 50 km long reach discretized by 1,135 cross-sections, obtained by interpolating the 274 cross-sections obtained by land survey: the reaches where the flow is supercritical (grey colour) and the positions of the 49 bridges and 11 diversion weirs (arrows) crossing the river are illustrated in Figure 14. This Figure clearly shows that transitions from sub- to supercritical flow and vice versa are very frequent.

Water level

All schemes provide at first sight a good estimate of the water elevation. However, closer looks reveal significant differences at some locations featuring strong variations of the topography. Four reaches (1.8–2.3, 23.0–24.0, 34.7–37.0 and 43.0–48.0 km) representative of the most difficult situations encountered in the river, are analysed in more detail. Results for the second and the third reach are illustrated in Figures 15(a) and 15(b).

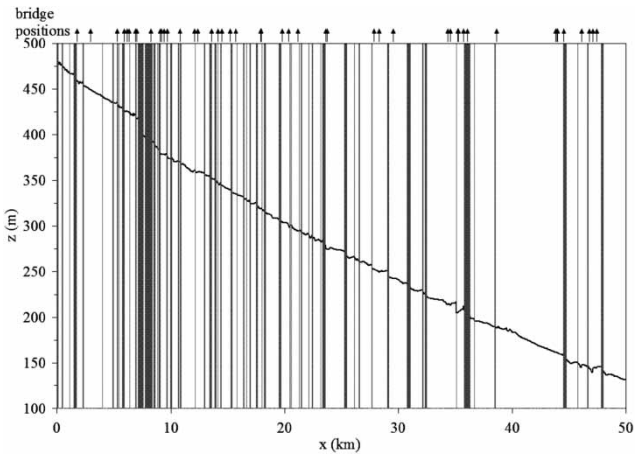

Figure 14 | Identification of the supercritical flow areas in the Brembo River for a discharge of 400 $m^3 s^{-1}$ (grey areas) and bridge positions (arrows).

In the above mentioned figures the critical elevation ($F = 1$) and the reference solution are also shown.

We note that SANA and CLHLL provide smooth solutions, while the HLL-CL scheme produces unphysical irregularities of the free-surface elevation, located where either bed elevation or cross-section width rapidly change.

In the reach shown in Figure 15(b), the check dam located at $x = 35.1$ km results in an abrupt lowering of the river bottom, followed by an adverse step; downstream the river maintains an almost critical slope. Following the reference solution, the water surface is almost horizontal in the pond downstream from the dam. This is reproduced by the finite-difference scheme SANA that however overestimates the water level, and predicts a wrong spilling of the water over the check dam, as illustrated by the sudden drop in water level. The HLL-CL scheme completely fails the simulation, while the CLHLL scheme provides results that are very close to the reference solution, with a realistic spilling over the check dam.

The results for all the schemes listed in Table 1 are given in Table 4 as the mean square error, in metres, between the reference solution and the scheme considered.

Dimensional errors are easily compared with the 1.00 m hydraulic freeboard of the Brembo River. The mean square errors listed in Table 4 are lower than 1 m, but in some locations errors exceed the prescribed hydraulic freeboard, as shown in Table 5.

Discharge

Discharges computed by SANA, HLL-CL and CLHLL schemes are illustrated in Figure 16. The discharge computed by the finite-volume schemes is far from being constant. SANA on the other hand reproduces the prescribed value of 400 $m^3 s^{-1}$.

The different behaviours of the finite-volume and finite-difference schemes can be explained as follows. In the finite-volume discretization of the shallow-water

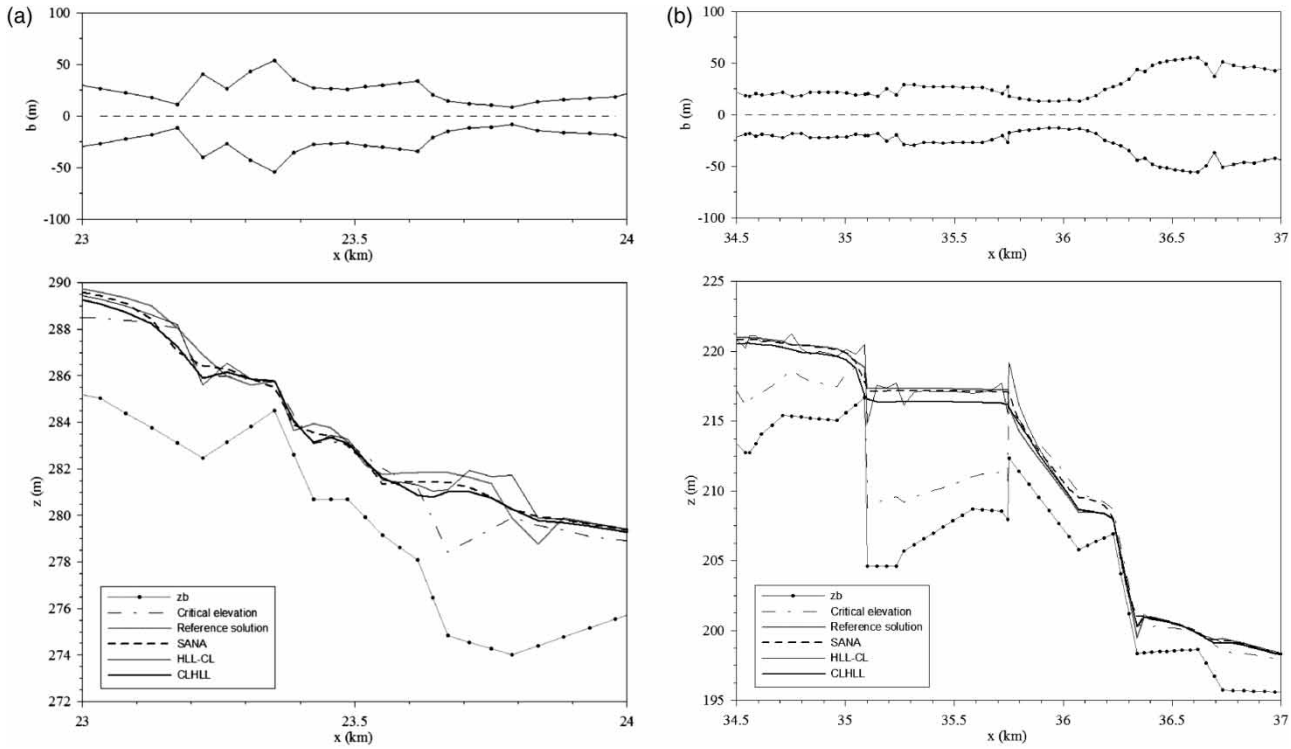

Figure 15 | (a) Longitudinal profile from $x = 23$ km to 24 km; above: width variation. (b) Longitudinal profile from $x = 34.7$ km to 37 km.

Table 4 | Brembo River. Mean square error of the computed water elevations (in metres)

Reach	Length	SANA	HLL-CL	CLHLL
1	km 1.8–km 2.3	0.493	0.744	0.581
2	km 23.0–km 24.0	0.446	0.622	0.508
3	km 34.7–km 37.0	0.431	0.765	0.528
4	km 43.0–km 48.0	0.259	0.375	0.282

Table 5 | Brembo River. Maximum error of the computed water elevations (in metres)

Reach	Length	SANA	HLL-CL	CLHLL
1	km 1.8–km 2.3	1.333	−1.526	0.950
2	km 23.0–km 24.0	1.166	1.847	1.099
3	km 34.7–km 37.0	1.560	3.293	−1.932
4	km 43.0–km 48.0	1.644	1.188	−1.491

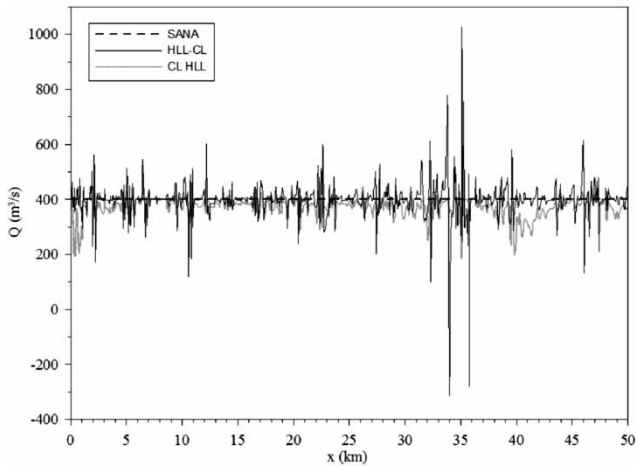

Figure 16 | Discharge profile for the entire Brembo River.

equations the variable Q_i shown in Figure 16 is evaluated to conserve the momentum or specific force in the discrete form of Equations (1) and (2). This value is generally different from the discharge that flows from one computational cell to another, which is calculated as the flux $Q^*_{i+1/2}$ in the discrete mass balance Equation (16). As a result the discharge value computed as Q_i is irregular since it is strongly influenced by the topographical source terms which depend on cross-section variation that can be strong in very irregular valleys. Clearly this is not the case for a

simple and smooth topography. The mass flux $Q^*_{i+1/2}$ on the other hand that represents the discharge computed between the computational cells, does not present this problem even for the finite volume schemes, as illustrated in Figure 17.

Total head

Even though the energy grade line should decrease in the downstream direction, the calculated total head sometimes increases owing to errors in computing water elevations and, mainly, water discharges. In particular, SANA wrongly computes reversed total head 76 times, HLL-CL 127 times, and CLHLL 76 times, almost at the same locations than SANA.

BREMBO RIVER CASE STUDY: 2003 FLOOD SIMULATION

The propagation of the 25th June 2003 flood wave along the Brembo river, having an estimated return period of 50 years, was simulated with HLL-CL, CLHLL and SANA schemes, using the boundary conditions defined above. This introduced set of 1,134 cross-sections including 49 bridge sections (shown in Figure 14) was used.

In the present work the bridge piers were added in the cross-section geometry. In all the performed simulations the bridges were never overtopped. However, future work will focus on bridges and the way to include them maybe more efficiently in numerical simulations as already introduced by some of the authors in (Natale *et al.* 2004).

The water mark elevations surveyed soon after the passage of flood are compared to the water elevations envelopes: the general agreement is good. Looking into the details, Figures 18 and 19 show that at some locations the numerical model does not reproduce correctly the flood marks, mainly in the critical reaches that already posed some difficulties in the steady-flow case.

Figures 18 and 19 show a good agreement between measurements and simulations, for all the proposed schemes.

CONCLUSIONS

Generally, the studies of flood wave propagation in natural rivers consider almost regular geometries, even though the majority of water courses in the densely populated European mountain valleys present very uneven topographies.

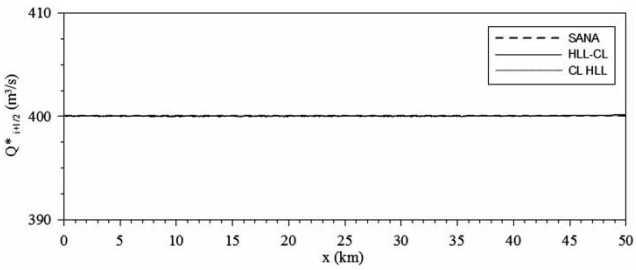

Figure 17 | Mass flux profile for the entire Brembo River.

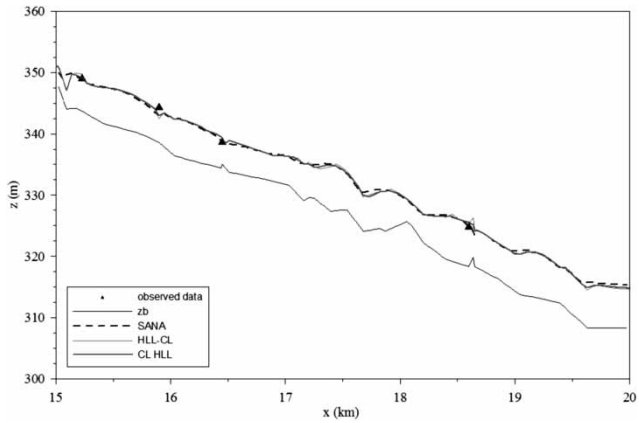

Figure 18 | Water elevation between $x = 15$ km and $x = 20$ km.

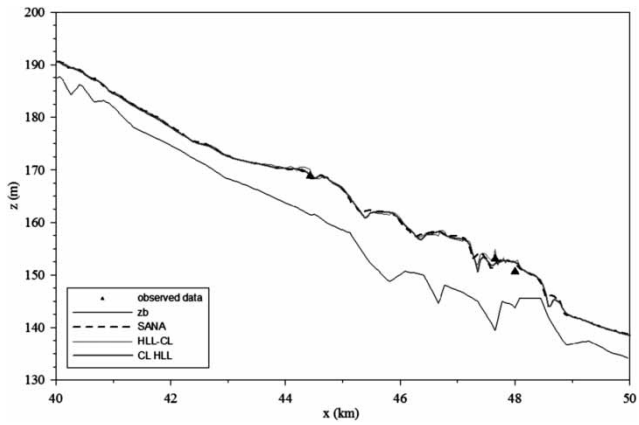

Figure 19 | Water elevation between $x = 40$ km and $x = 50$ km.

Based on a first series of test cases with analytical solutions, it could be shown that: (i) a coupled formulation of the topographical source terms is best suited for accurate water level predictions on variable topographies; (ii) for finite-volume schemes, discharge predictions should be based on the mass flux Q^* of the flux vector $F^*(\mathbf{U})$ rather than on the variable Q in the vector $\mathbf{U}$ of conserved variables; and (iii) in finite-volume scheme, the lateralization of the topographical source terms, written in terms of the coupled formulation, produces smooth water surfaces instead of unrealistic discontinuities.

Then, the authors considered the results of the 1D models tested on a real challenging case: the Brembo River, an Alpine water course characterized by steep slopes, abrupt cross-section changes and hydraulic singularities. The study of the Brembo River, first under steady flow conditions then in an unsteady case, demonstrated that the numerical simulations are not always accurate and consistent.

When a reduced number of land surveyed river sections is available, the unevenness of river-bed geometry is artificially emphasized and the application of 1-D numerical schemes becomes more difficult. To overcome the problem, the river-bed variations are usually smoothed including some interpolated sections between the surveyed ones; thus creating an artificial geometry. However, even though the sections are smoothed, the finite volume numerical schemes are not able to reproduce realistic results in the discharge profiles. Only the representation of the mass flux Q^* of the flux vector $F^*(\mathbf{U})$ is applicable to real word cases.

Finally, conclusions drawn from the Brembo River application, support and enhance the conclusions from the test cases with analytical solutions. Application of the proposed CLHLL scheme to the 2003 flood showed not only a good agreement to the few available measured water levels, but also realistic results all over the valley. For practical applications the use of the mass flux has to be preferred to the discharge.

ACKNOWLEDGEMENTS

The work described in this publication was partly supported by the European Community's Sixth Framework Programme through the grant to the budget of the Integrated Project FLOOD*site*, Contract GOCE-CT-2004-505420. This document reflects only the authors' views and not those of the European Community. The authors also would like to acknowledge the support of the CGRI-FNRS (Belgium) and the Ministero degli Affari Esteri Italiano (MAE, Italy) for the 2007–2008 project 'Engineering application of flood simulation techniques'. The data used in this paper are available by contacting *petaccia@unipv.it*.

REFERENCES

Abbott, M. B. & Ionescu, F. 1967 On the numerical computation of nearly horizontal flows. *Journal of Hydraulic Research* **5**, 97–117.

Alcrudo, F. & Garcia Navarro, P. 1992 Flux difference splitting for 1D open channel flow equations. *International Journal of Numerical Methods in Fluids* **14**, 1009–1018.

Arcement, G. J. & Schneider, V. R. 2001 Guide for selecting manning's roughness coefficients for natural channels and flood plains. U. S. geological survey. *Water Supply*, Paper 2339.

Aricò, C. & Tucciarelli, T. 2007 A marching in space and time (MAST) solver of the shallow water equations. Part I, the 1D model. *Advances in Water Resources* **30**, 1236–1252.

Bermudez, A. & Vasquez, M.E. 1994 Upwind methods for hyperbolic conservation laws with source terms. *Computers and Fluids* **23**, 1049–1071.

Brunner, G. W. 2002 *HEC-RAS River Analysis System Hydraulic Reference Manual, Version 3.1*. Hydrologic Engineering Center, Institute for Water Resources, US Army Corps of Engineers, Davis, CA.

Caleffi, V., Valiani, V. & Bernini, A. 2006 Fourth-order balanced source term treatment in central WENO schemes for shallow water equations. *Journal of Computational Physics* **218**, 228–245.

Capart, H., Eldho, T. I., Huang, S. Y., Young, D. L. & Zech, Y. 2003 Treatment of natural geometry in finite volume river flow computations. *Journal of Hydraulic Engineering* **129**, 385–393.

Cunge, J. A., Holly, F. M. & Vervey, A. 1980 *Practical Aspects of Computational River Hydraulics*. Pitman Publ. Inc., London.

Finaud-Guyot, P., Delenne, C., Lhomme, J., Guinot, V. & Llovel, C. 2010 An approximate-state Riemann solver for the two-dimensional shallow water equations with porosity. *International Journal for Numerical Methods in Fluids* **62**, 1299–1331.

Fraccarollo, L., Capart, H. & Zech, Y. 2003 A Godunov method for the computation of erosional shallow water transients. *International Journal for Numerical Methods in Fluids* **41**, 951–976.

Garcia Navarro, P., Fras, A. & Villanueva, I. 1999 Dam-Break flow simulation: some results for one dimensional models of real cases. *Journal of Hydrology* **216**, 227–247.

Garcia Navarro, P. & Vasquez Cendon, M. E. 2000 On numerical treatment of the source terms in the shallow water equations. *Computers and Fluids* **29**, 951–979.

Glaister, P. 1993 Flux difference splitting for open-channel flows. *International Journal for Numerical Methods Fluids* **16**, 629–654.

Greenberg, J. M. & Leroux, A. Y. 1996 A well-balanced scheme for the numerical processing of source terms in hyperbolic equations. *SIAM Journal on Numerical Analysis* **33**, 1–16.

Godunov, S. K. 1959 A finite difference method for the computation of discontinuous solutions of the equations of fluid dynamics. *Mat. Sb.* **47**, 357–393.

Goutal, N. & Maurel, F. 1997 Editors. Proceedings of the second workshop on dam-break wave simulation. Technical Report HE-43/97/016. Laboratoire National d'Hydraulique Chatou, Electricité de France.

Harten, A., Lax, P. D. & Van Leer, B. 1983 On upstream differencing and Godunov type schemes for hyperbolic conservation laws. *SIAM Review* **25**, 35–61.

He, H., Yu, Q., Zhou, J., Tian, Y. Q. & Chen, R. F. 2008 Modeling complex flood flow evolution in the middle yellow river basin, China. *Journal of Hydrology* **353**, 76–92.

Helmio, T. 2005 Unsteady 1D flow model of a river with partially vegetated floodplains- application to the Rhine River. *Environmental Modeling & Software* **20**, 361–375.

Hirsh, C. 1992 *Numerical Computation of Internal and External Flows*. John Wiley & Sons, Chicester.

Hubbard, M. E. & Garcia Navarro, P. 2000 Flux difference splitting and the balancing of source terms and flux gradients. *Journal of Computer Physics* **165**, 89–125.

Kuiry, S. N., Pramanik, K. & Sen, D. 2008 Finite volume model for shallow water equations with improved treatment of source terms. *Journal of Hydraulic Engineering* **134**, 231–242.

Lee, S. H. & Wright, N. G. 2010 Simple and efficient solution of the shallow water equations with source terms. *International Journal for Numerical Methods Fluids* **63**, 313–340.

LeVeque, R. J. 1998 Balancing source terms and flux gradients in high-resolution Godunov methods: the quasi-steady wave-propagation algorithm. *Journal of Computational Physics* **146**, 346–365.

Lhomme, J. & Guinot, V. 2007 A general approximate-state Riemann solver for hyperbolic systems of conservation laws with source terms. *International Journal for Numerical Methods Fluids* **53**, 1509–1540.

Liang, Q. & Marche, F. 2009 Numerical resolution of well-balanced shallow water equations with complex source terms. *Advances in Water Resources* **32**, 873–884.

Mahmood, K. & Yevjevich, V. 1975 *Unsteady Flow in Open Channels*. Water Resources Publication, Fort Collins, CO.

Natale, L. & Savi, F. 1992 Propagazione di onde di sommersione in un canale vuoto. Proc. Jornadas de Encuentro Trilateral para el estudio de la idraulica de las ondas de submersion, Zaragoza, 46–77. (In Italian.)

Natale, L. & Savi, F. 1999 *Manuale di Frescure*. Internal report. Università degli Studi di Pavia, Dipartimento di Ingegneria idraulica e Ambientale, Pavia. (In Italian.)

Natale, L., Petaccia, G. & Savi, F. 2004 Simulation of dam-break waves propagation in rivers with bridges and structures. *Proceedings of the International Conference in Fluvial Hydraulics Riverflow 2004* **2**, 895–901.

Nujic, M. 1995 Efficient implementation of non-oscillatory schemes for the computation of free surface flows. *Journal of Hydraulic Research* **33**, 101–111.

Petaccia, G. & Savi, F. 2002 Numerical modelling of shock waves: simulation of a large number of laboratory experiments. *Proceedings of the International Conference in Fluvial Hydraulics, Riverflow 2002* **1**, 449–458.

Pu, J. H., Cheng, N., Tan, S. K. & Shao, S. 2012 Source term treatment of SWEs using surface gradient upwind method. *Journal of Hydraulic Research* **1**, 1–9.

Remo, J. W. F. & Pinter, N. 2007 Retro-modeling the Middle Mississippi River. *Journal of Hydrology* **337**, 421–435.

Roe, P. L. 1981 Approximate Reimann solvers, parameter vectors, and difference schemes. *Journal of Computational Physics* **43**, 357–372.

Roe, P. L. 1987 Upwind differencing schemes for hyperbolic conservation laws with source terms. *Nonlinear Hyperbolic Problems*. Springer, Berlin/Heidelberg, vol. 1270, pp. 41–51.

Savic, L. J. & Holly Jr., F. M. 1993 Dam break flood waves computed by modified Godunov method. *Journal of Hydraulic Research* **31**, 187–204.

Schippa, L. & Pavan, S. 2008 Analytical treatment of source terms for complex channel geometry. *Journal of Hydraulic Research* **46**, 753–763.

Sielecki, A. 1968 An energy conserving difference scheme for the storm surge equations. *Monthly Weather Review* **96**, 150–156.

Soares-Frazão, S. 2002 Dam-break induced flows in complex topographies - Theoretical, numerical and experimental Approaches. PhD thesis, Université catholique de Louvain, Belgium.

Soares-Frazão, S., Morris, M. & Zech, Y. 2000 CADAM Concerted Action on Dam Break Modeling: Objectives, Project Report, Test Cases, Meeting Proceedings. Université catholique de Louvain, Civ. Eng. Dept., Hydraulics Division, Louvain-la-Neuve, Belgium. CD-ROM.

Toro, E. F. 2001 *Shock Capturing Methods for Free Surface Shallow Flows*. Wiley, Chicester.

Toro, E. F. 2009 *Riemann Solvers and Numerical Methods for Fluid Dynamics*. Springer, Berlin.

Tseng, M. H. 2004 Improved treatment of source terms in TVD scheme for shallow water equations. *Advances in Water Resources* **27**, 617–629.

Valiani, V., Caleffi, V. & Zanni, A. 2002 Case study: Malpasset dam-break simulation using a two-dimensional finite volume method. *Journal of Hydraulic Engineering* **128**, 460–472.

Vazquez-Cendon, M. E. 1999 Improved treatment of source terms in upwind schemes for shallow water equations in channels with irregular geometry. *Journal of Computational Physics* **148**, 497–526.

Vignoli, G., Titarev, V. A. & Toro, E. F. 2008 ADER schemes for the shallow water equations in channel with irregular bottom elevation. *Journal of Computational Physics* **227**, 2463–2480.

Vukovic, S. & Sopta, L. 2003 Upwind schemes with exact conservation property for one-dimensional open channel flow equations. *SIAM Journal on Science Computing* **24**, 1630–1649.

Xing, Y. & Shu, C. W. 2011 High order finite volume WENO schemes for the shallow water equations with dry states. *Advances in Water Resources* **34**, 1026–1038.

Ying, X., Khan, A. A. & Wang, S. S. Y. 2004 Upwind conservative scheme for the Saint Venant equations. *Journal of Hydraulic Engineering ASCE* **130**, 977–987.

Ying, X. & Wang, S. S. Y. 2008 Improved implementation of the HLL approximate Riemann solver for one-dimensional open channel flows. *Journal of Hydraulic Research* **46**, 21–34.

Yoshida, H. & Dittrich, A. 2002 1D unsteady state flow simulation of a section of the upper Rhine. *Journal of Hydrology* **269**, 79–88.

Wang, J. S., Ni, H. G. & He, Y. S. 2000 Finite-difference TVD scheme for computation of dam-break problems. *Journal of Hydraulic Engineering* **126**, 253–262.

Wang, Y., Liang, Q., Kesserwani, G. & Hall, J. W. 2011 A 2D shallow flow model for practical dam break simulations. *Journal of Hydraulic Research* **49**, 307–316.

Wright, N. G., Villanueva, I., Bates, P. D., Mason, D. C., Wilson, M. D., Pender, G. & Neelz, S. 2008 Case study of the use of remotely sensed data for modeling flood inundation on the river Severn, U.K. *Journal of Hydraulic Engineering* **134**, 533–540.

Zhou, G., Causon, D. M., Mingham, C. G. & Ingram, D. M. 2001 The surface gradient method for the treatment of source terms in the shallow-water equations. *Journal of Computational Physics* **168**, 1–25.

First received 14 September 2011; accepted in revised form 11 May 2012. Available online 12 July 2012